

Electronic Flow Control Valve (EFCV) with Pressure Compensation Capability

QingHui Yuan (Eaton Corporation)

Innovation Center, Eaton Corporation, Eden Prairie, MN USA

Chris Schottler (Eaton Corporation)

Hydraulics Division, Controls Group, Eden Prairie, MN USA

Jae Y.Lew (Eaton Corporation)

Innovation Center, Eaton Corporation, Eden Prairie, MN USA

ABSTRACT

A new concept for an Electronic Flow Control Valve (EFCV) with pressure compensation capability is introduced. Based on its embedded sensors and micro controller, the EFCV can provide flow control without the need of load/displacement/speed information from the power elements, like hydraulic cylinders or hydraulic motors. The flow controller inside the EFCV estimates the actual flow rate by the quasi-steady flow rate equation. Experimental studies show that the analytical model is not accurate enough to cover all operating conditions. Therefore, an experiment-based calibration method is suggested so that the electronic flow controller can provide accurate flow control across the working pressure and flow range. Finally, an innovative application of the EFCV, a self-sensing cylinder, is also presented.

NOMENCLATURE

A	Cap area of the spool	m^2
A_1	Piston area of cylinder	m^2
F_{vc1}	Force produced by the voice coil	N
$F_{sp1} F_{s1}$	Steady flow forces for pilot and main stage	N
$K_{correction}$	Error-correction coefficient	
$K_{sp} K_s$	Centering spring constant for pilot and main stage	N/m
$K_{vp} K_v$	Damping coefficient for the pilot and main stage	Ns/m
$M M_m$	Spool mass for pilot and main stage	K_g
P_1, P_2	Port pressure	P_a
P_{11}, P_{12}	Chamber pressures.	P_a
P_s	Supply pressure	P_a
P_t	Return pressure	P_a
Q_1, Q_2	Port flow rate	m^3/s
Q_{11}	Flow rate into the upper chamber	m^3/s
Q_{12}	Flow rate out of the lower chamber	m^3/s
$Q_{1,d} Q_{1,c} Q_{1,m}$	Desired/calculated/measured flow rate	m^3/s
V_o	Volume of chamber 1 as $x_p = 0$	m^3
$V_{11} V_{12}$	Volumes in the upper and lower chamber	m^3
$W_p W$	Area gradient for the pilot and main stage	m
i	Current through the actuator coil	A
$x_1 x_{v1}$	Spool displacement for pilot and main stage	m
x_p	Piston displacement	m
β_e	Bulk modulus of hydraulic fluid	Pa

1.0 INTRODUCTION

Flow control is one of the most critical functionalities in the hydraulic industry. Traditionally, flow control is implemented via a proportional or servo valve. The principle of proportional and servo valves is briefly reviewed in the following. When current is applied into the coil of a solenoid (proportional valve) or a torque motor (servo valve), a corresponding electromagnetic force is generated. These forces could either directly stroke the spool (single stage configuration) or indirectly move the main stage spool via regulating the hydraulic pressures on the each end of the main stage spool (multiple stage configuration). The motion of the main stage spool leads to the variation of the orifice area. With a given pressure drop, the orifice area is directly associated with the flow rate. Modeling and control of proportional and servo valves is very rich in literature /Mer67/Jel03/Eat99/. However, most proportional and servo valves on the market are incapable of providing accurate flow rate control without feedback from the power elements or without the addition of mechanical pressure compensators. For example, consider a double-ended hydraulic cylinder with the piston area equal to 1 [unit]. If the required speed is 1 [unit], then the required flow rate is actually 1 [unit]. Without knowing the displacement/speed information from the hydraulic cylinder, neither the servo valve nor the proportional valve can correctly provide the desired flow. The reason for this is because the flow rate is related not only to the spool displacement (orifice area) but also to the pressure drop across the orifice. Therefore, feedback from the power elements is often required to achieve accurate flow control.

In real world applications, the sensors in the power elements are not often available or are too costly to implement. However, accurate flow control is still required for several applications. For example, in a mobile excavator application the operators are in the loop controlling the motion of machine. The operators use a human machine interface device (like a joystick) to send the flow command to each individual cylinder. By controlling the angle of the joystick on each axis, one may also control the speed of multiple cylinders. Despite the variance in supply pressure of the system and the changing loads on the power elements, it is preferred that a joystick angle provides a corresponding velocity of the cylinder/motor consistently.

The traditional solution for this problem is to regulate the pressure drop across the metering orifice to be constant, so that the flow rate is essentially only dependent on the orifice area. This is the principle of a pressure-compensated flow control valve. **Figure 1** illustrates a typical restrictor-type pressure-compensated flow control valve /Eat99/. The compensator spool has to be added to implement pressure regulation functionality. This methodology adds additional cost and complexity to the system.

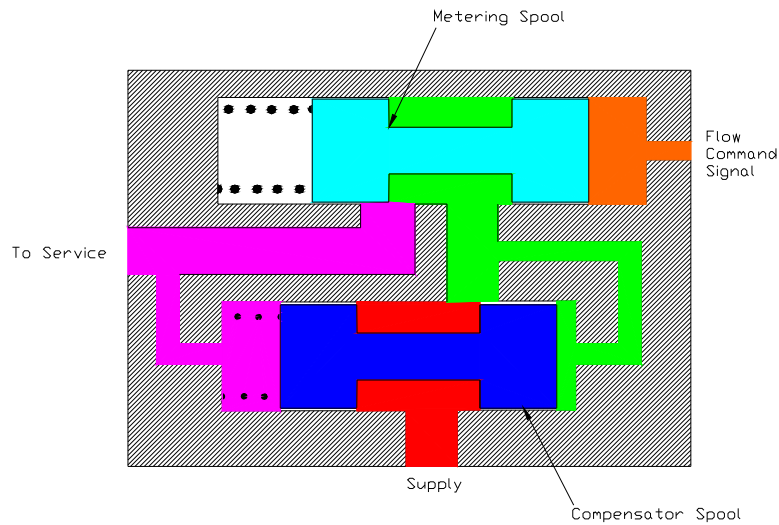


Figure 1 Restrictor-type pressure-compensated flow control valve

In the following paper, an innovative flow control valve with pressure compensation capability, referred to as an Electronic Flow Control Valve (EFCV), is presented. The EFCV distinguishes itself from other traditional flow control valves because of its embedded sensors and micro controller that have been integrated in to the valve. These integrated components make the EFCV “smart” so it can achieve flow control without the need of feedback from the power elements or the addition of a complicated mechanical system to regulate the pressure drop across the metering orifice. The Electronic Pressure Compensated Flow Control Valve is more cost effective and scalable compared to its mechanical counterparts.

The paper is organized as follows. First, the configuration and model of EFCV is developed. Next, the principle of electronic flow control via the EFCV integrated controller is described. Subsequently, the experimental study regarding the flow control accuracy is reviewed. Finally, an application of EFCV for a self-sensing cylinder is presented as well as some concluding remarks.

2.0 ELECTRONIC FLOW CONTROL VALVE

2.1 System Configuration

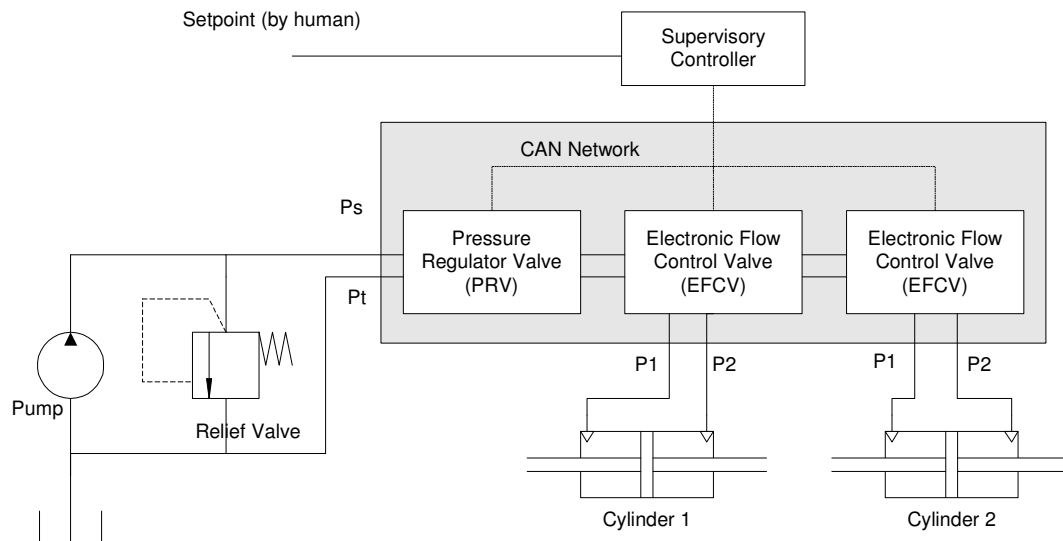


Figure 2 Configuration of hydraulic system with Electronic Flow Control Valve (EFCV)

Figure 2 illustrates the system design of the EFCV. A supervisory controller, which is implemented by an ECU, processes the input from the human as the set point for the flow rate. An EFCV, as well as a Pressure Regulation Valve (PRV), are connected to the supervisory controller via CAN communication. The embedded sensors in the PRV can provide the value of the supply pressure (P_s), and the tank pressure (P_t). The PRV can also control the supply pressure according to the load requirement, which is out of scope for this paper. The embedded sensors in the EFCV include the LVDTs, which measure the main stage spool displacement, and the pressure sensors, which measure the port pressures P_1 and P_2 . The ports P_1 and P_2 are connected with hydraulic power elements as shown in **Figure 2**. It is worth mentioning that the system is designed so that multiple EFCVs may be connected with multiple power elements. Finally, the entire valve stack, including PRV and EFCVs, are connected to the hydraulic source (pump and a relief valve as shown in **Figure 2**).

The differentiating characteristic of the EFCV when compared to servo and proportional valves is the pressure feedback from the internal sensors. The pressure feedback combined with the positional feedback from the main stage spool, allows the EFCV to control the flow rate based on the command from the supervisory controller. On the contrary, traditional servo and proportional valves do not have internal pressure feedback inside the valves themselves and therefore cannot accurately control the flow rate across a large pressure drop spectrum.

2.2 Internal model of EFCV

An illustration of the pilot and main-stage spools in the EFCV is shown in **Figure 3**. It is important to note that for complete control of a typical power element, an additional pilot and main-stage spool is required. The embedded electronics performs the internal control, the communication between individual valves, and the communication to the supervisory controller. The EFCV has a two-stage configuration. The pilot stage, stroked by a linear force motor (voice coil), can control the pressures on the end chambers of the main stage spool while the main stage spool can then control the flow rate to the power element. In addition, the EFCV can be designed to have independent upstream and downstream orifice control for the sake of energy savings and application flexibility. The schematic in **Figure 3** only reflects the configuration of the upstream or downstream portion of the EFCV. Interested readers may refer to /Eat92/ for more details about twin spool valves.

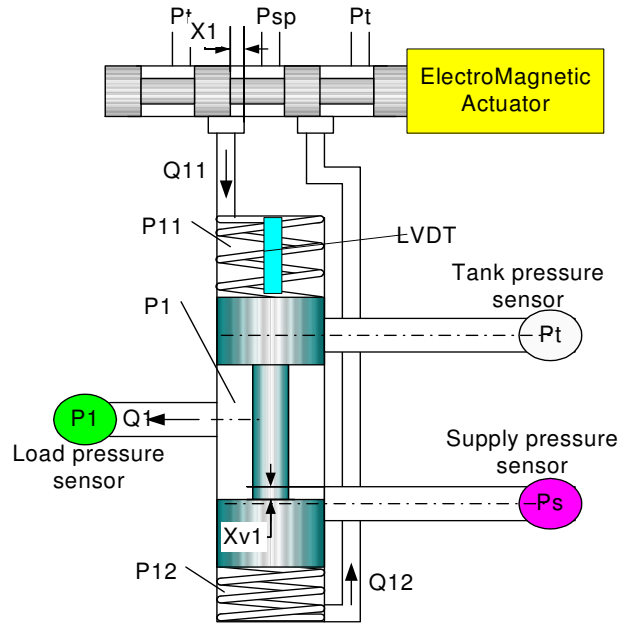


Figure 3 Schematic of Electronic Flow Control Valve (EFCV)

In the next section, the models of the EFCV related to the flow control will be developed.

2.3 EFCV model

2.3.1 Pilot stage spool dynamics

We assume that the transient flow forces applied on the pilot spool are negligibly small. From Newton's Second Law, we have the spool dynamics as follows:

$$M\ddot{x} = F_{vc1} + F_{sp1} - K_{vp}\dot{x}_1 - K_{sp}x_1 \quad (1)$$

in which M is the pilot spool mass, F_{vc1} is the force produced by the voice coil, which is proportional to the current i driven through the actuator coil, K_{sp} is the centering spring constant, and F_{sp1} is the steady state flow induced forces that are governed by:

$$F_{sp1}(x_1, P_{11}, P_{12}) = \begin{cases} -2C_d W_p x_1 \cos \theta [P_{sp} - P_t - (P_{11} - P_{12})], & x_1 \geq 0; \\ -2C_d W_p x_1 \cos \theta [P_{sp} - P_t - (P_{12} - P_{11})], & x_1 < 0. \end{cases} \quad (2)$$

where C_d is the discharge coefficient, W_p is the gradient area for the pilot stage, θ is the jet angle, P_{sp} is the supply pressure for the pilot stage, and P_t is the pressure of the reservoir. P_{11} and P_{12} are the chamber pressures shown in **Figure 2**. The viscous damping coefficient, K_{vp} , can be computed based on the valve geometry via /Mer67/.

2.3.2 Main stage dynamics

Similarly, the main stage spool dynamics can be obtained:

$$M_m \frac{d}{dt} \dot{x}_{v1} = -K_s x_{v1} - K_v \dot{x}_{v1} + (P_{11} - P_{12})A + F_{s1} \quad (3)$$

where M_m is the spool mass in the second stage, x_{v1} is the displacement of the spool, K_s is the centering spring constant, K_v is the viscous damping coefficient, A is the cap area of the spool contacting the end chambers, P_{11} and P_{12} are the chamber pressures. F_{s1} is the steady state flow force.

The steady state flow force, F_{s1} is given by:

$$F_{s1}(x_{v1}) = \begin{cases} -2C_d W x_{v1} \cos \theta (P_s - P_1), & x_{v1} \geq 0; \\ -2C_d W x_{v1} \cos \theta (P_1 - P_t), & x_{v1} < 0. \end{cases} \quad (4)$$

where W is the area gradient for the main stage, P_s is the supply pressure, and the other variables can be referenced from Eq. (2).

2.3.3 Chamber pressure dynamics

The chamber pressure dynamics are determined by the compressibility of the fluid in the chambers between the pilot stage and the main stage spools and are as follows:

$$\frac{d}{dt} P_{11} = \frac{\beta_e}{V_{11}} (Q_{11} - A \dot{x}_{v1}) \quad (5)$$

$$\frac{d}{dt} P_{12} = \frac{\beta_e}{V_{12}} (A \dot{x}_{v1} - Q_{12}) \quad (6)$$

in which P_{11} and P_{12} are the pressures in the upper and lower chambers, respectively, Q_{11} is the flow rate into the upper chamber, Q_{12} is the flow rate out of the lower chamber, β_e is the bulk modulus of hydraulic fluid, V_{11} and V_{12} are the volumes in the upper and lower chamber. On the quasi-steady state flow assumption, Q_{11} and Q_{12} are given by:

$$Q_{11}(x_1, P_{11}) = \begin{cases} C_d W_p x_1 \sqrt{2(P_{sp} - P_{11})/\rho}, & x_1 \geq 0; \\ C_d W_p x_1 \sqrt{2(P_{11} - P_t)/\rho}, & x_1 < 0. \end{cases} \quad (7)$$

$$Q_{12}(x_1, P_{12}) = \begin{cases} C_d W_p x_1 \sqrt{2(P_{12} - P_t)/\rho}, & x_1 \geq 0; \\ C_d W_p x_1 \sqrt{2(P_{sp} - P_{12})/\rho}, & x_1 < 0. \end{cases} \quad (8)$$

2.4 Flow Control of EFCV

The above model shows the EFCV is a highly nonlinear system with six states. However, a reduced model can be obtained from the following facts:

1. The pilot stage has very fast response. Compared to the other dynamics within the system, the transfer function from the current (i) to the pilot spool displacement (x_1) can be simplified as a DC gain.
2. Next, the transfer function of the main stage from x_1 to x_{v1} can be written as

$$\frac{x_{v1}(s)}{x_1(s)} = \frac{\frac{2\beta_e K_{qp} A}{V_0}}{s[M_m s^2 + K_v s + (\frac{2\beta_e A^2}{V_0} + K_2)]} \quad (9)$$

where $K_2 = K_s + C_d W \cos \theta (P_s - P_t)$, $K_{qp} = C_d W_p \sqrt{\frac{P_{sp} - P_t}{\rho}}$. In our analysis, the transient flow forces are neglected. The linearized equation has poles located at 0 and are repeated at -160.

In short, the higher order system can be approximated by a second order system in series with an integrator. For this open-loop stable system, a standard PI controller is chosen to assure adequate performance of the closed loop system. Standard PI gain tuning techniques can be used /Lev96/.

The flow control diagram is illustrated in **Figure 4**. The desired flow rate $Q_{1,d}$ is given by the supervisory controller thru the CAN bus. The actual flow rate $Q_{1,c}$ is analytically given by /Mer67/:

$$Q_{1,c} = f(P_s, P_1) x_{v1} \quad (10)$$

where the flow mapping $f(P_s, P_1) = \begin{cases} C_d W x_{v1} \sqrt{2(P_s - P_1)/\rho}, & x_{v1} > 0 \\ C_d W x_{v1} \sqrt{2(P_1 - P_t)/\rho}, & x_{v1} \leq 0 \end{cases}$.

In the diagram, the inverse flow mapping is used to convert the desired flow rate $Q_{1,d}$ to the desired spool displacement $x_{v1,d}$. The error between the desired and the actual displacement is imposed on the PI controller, whose output will drive the current into the pilot valve voice coil. The controller drives the displacement error to zero. If the actual flow follows Eq. (10) perfectly, then the flow error goes to zero as well, or $Q_{1,c} = Q_{1,d}$. Otherwise, if the actual flow mapping $g(\cdot) \neq f(\cdot)$, or $f^{-1}g \neq 1$, then the flow error will not converge to zero even when the displacement error is zero. In the following section, we will investigate the flow rate accuracy experimentally.

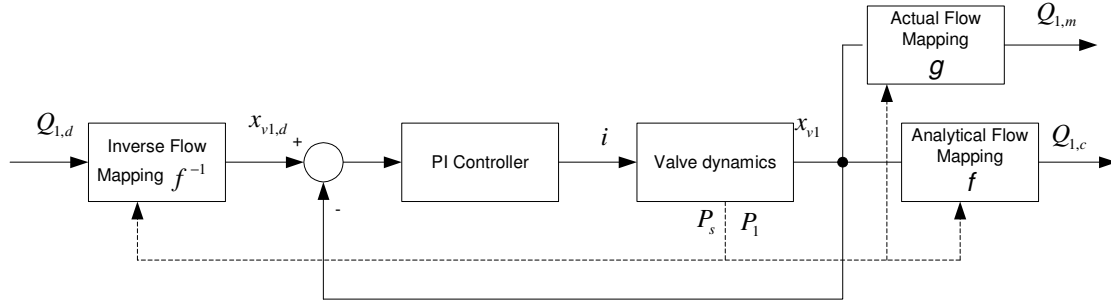


Figure 4 The flow control diagram inside EFCV

3.0 EXPERIMENTAL STUDY OF ELECTRONIC FLOW CONTROL

In the flow controller design, we use Eq. (10) to approximate the actual flow rate. Eq. (10) is a widely acceptable quasi-steady state model for the flow rate across an orifice. In the following section, an experimental study will be discussed that investigated the accuracy of the calculation.

A prototype of EFCV has been built and tested. The mechanical design can be referred to in **Figure 3**. The hydraulic test set up is illustrated in **Figure 5**. As you can see from Figure 5, the valve was set up on a fixed displacement test stand. An adjustable relief valve (on the right side of **Figure 5**) simulates a load on the valve. A flow meter in series with the “load” relief valve is used to measure the actual flow from that service. The type of flow meter that was used depends on the demanded flow in order to improve the measurement accuracy. For flows below 7 GPM a 0.95 in³/rev meter motor (Vickers Model MF3039133061592) was used; while for flows above 7 GPM a flow turbine was used (Max Machinery Model 241-120).

Given a flow command from the supervisory controller, the “load” relief valve is adjusted so that the pressure drop between P_1 and P_s is equal to some predefined value. Then the actual flow rate was measured. **Table 1** displays all of the actual flows [GPM] recorded as a function of the commanded flow [GPM] and the pressure drop [psi] across the service spool.

Note that at steady state, the PI controller in **Figure 4** regulates the error between the flow command $Q_{1,d}$ and the calculated flow rate $Q_{1,c}$ to be zero, or $Q_{1,d} = Q_{1,c}$ only if the flow mapping $f(\cdot)$ and the inverse flow mapping $f^{-1}(\cdot)$ are perfectly inverse. In **Table 1**, the experimental results show that the measured flow rate $Q_{1,m}$ diverts from the analytical calculation $Q_{1,c}$. Another source for the error could also be that the flow mapping is different from what we suggested, or $g(\cdot) \neq f(\cdot)$ as shown in **Figure 4**. For convenience, we will compare the measured flow rate $Q_{1,m}$ and the commanded flow rate $Q_{1,d}$ ($=Q_{1,c}$). The error

$\frac{Q_{1,m} - Q_{1,d}}{Q_{1,d}}$ (unit: %) as a function of the pressure drop is illustrated in **Figure 6**.

Remarks:

1. For small flow commands, the error is significant. For example, when $Q_{1,d} = 1.32$ [gpm], the actual flow rate only reaches about 20% of the demanded value. The error is larger than 80% at some pressure drops.
2. When the flow command is larger than 5 gpm, the error is bounded with $\pm 15\%$.
3. Given a flow command, the actual flow $Q_{1,m}$ first increases with the pressure drop. However, as the pressure drop is above 500-750 [psi], the flow $Q_{1,m}$ then reduces. This observation is based on the theoretical flow mapping $f(\cdot)$ in Eq. (10).

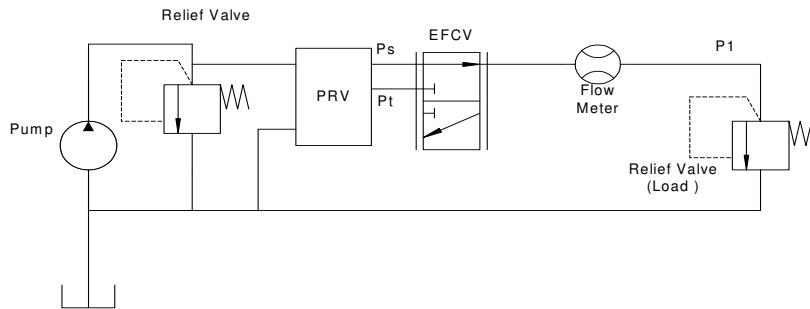


Figure 5 Diagram of the experimental setup

Command Flow	Differential Pressure [psi]									
	150	300	450	600	750	900	1000	1500	2000	2500
1.32	0.4	0.4	0.3	0.2	0.2	0.2	0.2	0.1	0.1	0.1
2.64	2.35	2.5	2.4	2.2	2.1	2	1.9	1.7	1.5	1.4
5	5	5.6	5.5	5.8	5.8	5.7	5.6	4.65	4.45	4.4
6.6	6.45	6.67	7.25	7.47	7.14	7.03	6.96	6.67	6.38	6.22
13.2	13.92	14.29	14.17	13.85	13.59	13.63	13.51	13.63	14.03	14.33
19.8	19.4	21.13	22.74	22.82	21.57	21.54	21.23	20.62	19.89	20.25
26.4	27.25	27.7	28.55	30.72	29.59	28.76	28.57	27.37	26.74	26.26
30.36	29.08	30.62	31.5	33.13	35.05	34.48	34.02	32.22	32.2	30.91

Table 1 Measured Flow $Q_{1,m}$ vs. Commanded Flow $Q_{1,d} (= Q_{1,c})$ (unit: GPM)

Obviously the observed error demonstrates that the flow rate model in Eq. (10) is not very precise. For simplicity, in our generation of the flow map we assumed the density (ρ) and the discharge coefficient C_d in Eq. (10) to be constant. In reality, the density of the fluid may vary slightly according to the pressure and will change proportionally with temperature. In addition, the discharge coefficient is a very complicated function with respect to the pressure drop, the orifice area, the orifice geometry, and the Reynolds number $Wu03/$. To precisely model (using CFD) the discharge coefficient for various operating conditions would be very difficult.

Due to the complexity of the discharge coefficient, a feasible and useful strategy is to experimentally calibrate the flow calculation equation to eliminate the theoretical error. An empirical error-correction coefficient, $K_{correction}$, is defined as:

$$K_{correction} = \arg \left[\min_K (\|Q_{1,c} - KQ_{1,m}\|) \right] \quad (11)$$

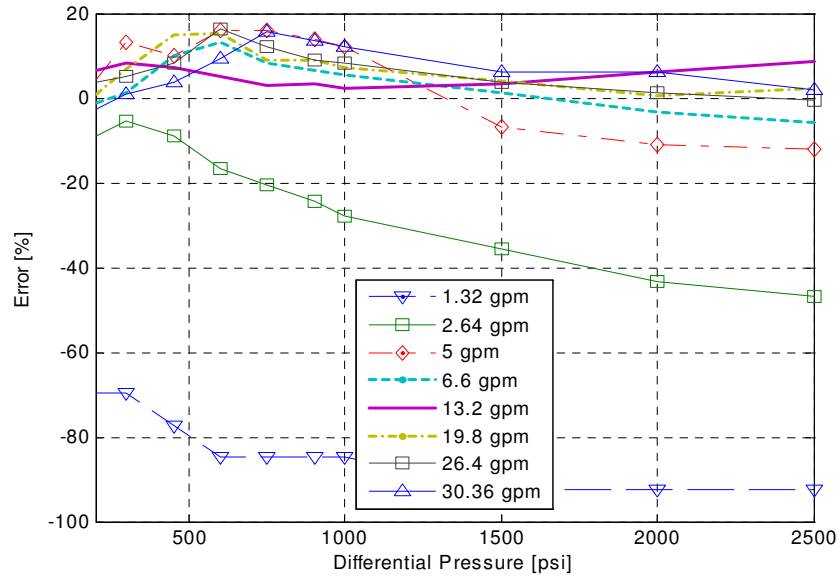


Figure 6 The error of the actual flow compared to the demanded flow, $\frac{Q_{1,m} - Q_{1,d}}{Q_{1,d}}$

The solution $K_{correction}$ is shown in **Figure 7**. The correction coefficient is a function of both pressure and flow rate. Curve fitting techniques can be used to get the relationship between $K_{correction}$ and the pressure drop and the flow rate. The following is an example that provides sufficient agreement with the measurement:

$$K_{correction} = c_0 + c_1x + c_2\sqrt{P} + c_3x^2 + c_4P \quad (12)$$

where $c_0=3.1387$, $c_1=-0.0085$, $c_2=-0.0383$, $c_3=-1.03e-5$, $c_4=9.13e-4$.

Due to the flexible system design of EFCV, the correction can be easily applied either inside EFCV or in the supervisory controller.

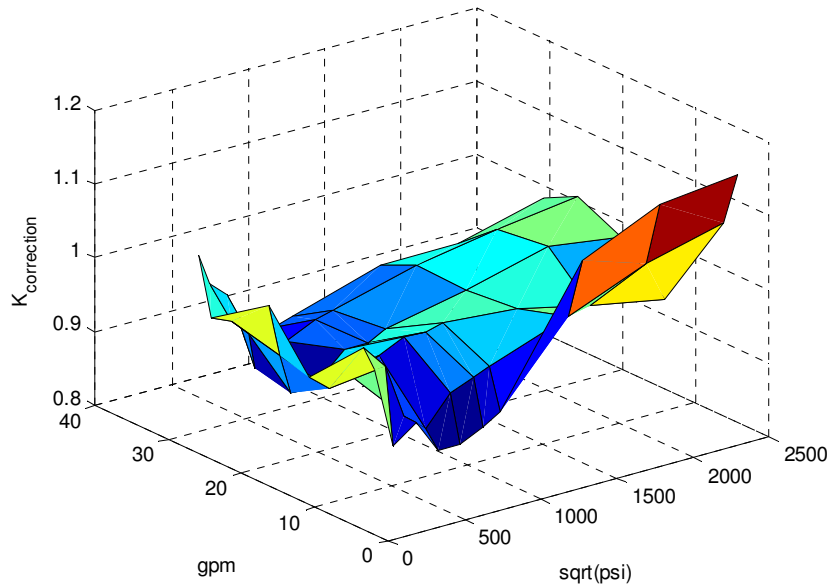


Figure 7 Correction gain for the flow rate calculation in Eq. (12)

4.0 APPLICATION OF EFCV: SELF-SENSING CYLINDER

In the following section we will discuss an innovative application for the EFCV. The application is a self-sensing cylinder, which will estimate the piston displacement of a regular hydraulic cylinder by taking advantage of integrated sensors and flow rate calculation of the EFCV.

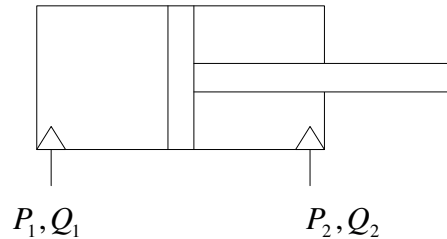


Figure 8 Self-sensing cylinder

The diagram of a self-sensing cylinder is illustrated in **Figure 8**. Two EFCVs connect each chamber respectively. The sensors in the EFCVs measure the pressures, P_1 and P_2 . The flow rates, Q_1 and Q_2 , are calculated by using the analytical model with the experimental calibration (as described above). In addition, in order to eliminate the integration error some deterministic displacement information is required (an absolute start position). For instance, a latch sensor could be installed so that the output voltage is high when the piston displacement $x_p = 0$ and is low as $x_p \neq 0$.

The pressure dynamics in chamber 1 gives

$$\dot{P}_1 = \frac{\beta_e}{V_0 + A_1 x_p} (Q_1 - A_1 \dot{x}_p) \quad (13)$$

where β_e is the bulk modulus of hydraulic fluid, V_0 is the volume of chamber 1 as $x_p = 0$, A_1 is the piston area, x_p is the piston displacement, and Q_1 is the calibrated flow rate.

By manipulating the above equation, an observer of the piston displacement is proposed as

$$\dot{x}_p = \frac{1}{\beta_e A_1} (-A_1 \eta_1 x_p - \eta_1 V_0 + \beta_e Q_1) \quad (14)$$

where $\eta_1 = P_1 \frac{s}{s+p}$, or the low pass filtering of the pressure differential.

The simulation results are shown below in **Figure 9**. Due to the combined effect of the flow rate and the load applied to the cylinder, the actual displacement is the sinusoidal signal with the higher frequency oscillation. The observer in Eq. (14) is a close approximation of the actual displacement. Note that at $t=0.1$ [sec], the latch sensor is enabled and then enforcing the error to be zero. Without the latch sensor, the observer will still give the similar displacement profile but with an offset error. In **Figure 9**, the estimate by using the simple kinematic relationship between the flow rate and the piston speed, $\dot{x}_p = \frac{Q_1}{A_1}$, is also plotted. It can be seen that its performance is worse than that in Eq. (14). In short, the integrated pressure sensors and the experimentally calibrated flow rates in the EFCV, together with the proposed observer, make it possible to implement the self-sensing cylinder.

CONCLUSION

A new type of valve, an Electronic Flow Control Valve (EFCV), is presented in this paper. Due to the embedded sensors and micro controller inside the valve, the flow rate can be controlled through the power elements without the need of knowing the load or the displacement condition from the power elements. The flow controller utilizes the well-known quasi-steady flow rate equation to approximate the actual flow rate in the internal closed loop system. Experimental studies show that the one equation model with constant parameters is not accurate enough to cover all conditions. In particular for the low flow rate high-pressure drop case, the flow error calculation is significant. An experiment-based calibration method is then presented. The new flow controller, by taking into account the error correction coefficient $K_{correction}$, could provide a very accurate flow controller. An innovative application of the EFCV, a self-sensing cylinder, is also described.

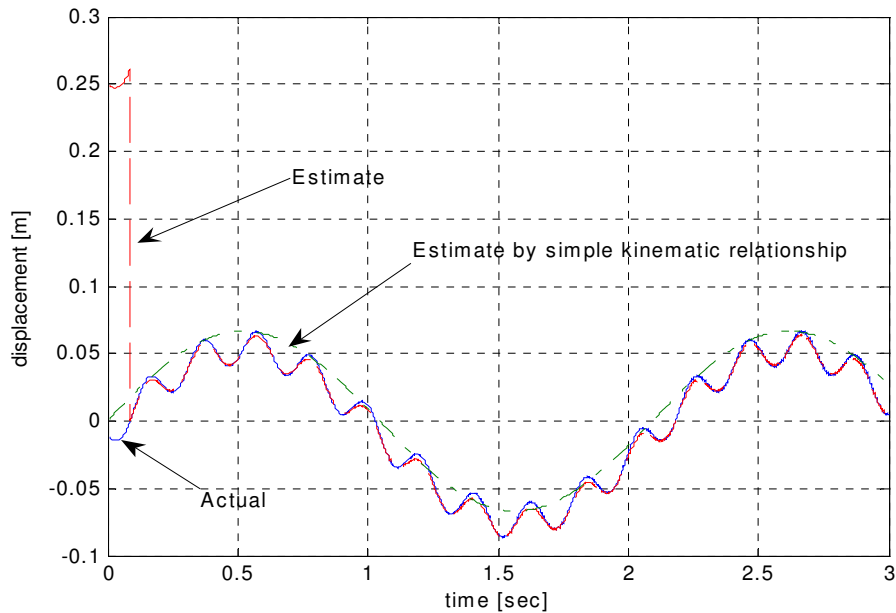


Figure 9 Simulation result: actual displacement and estimates

REFERENCES

- /Mer67/ **Herbert E Merritt**, Hydraulic control system, John Wiley and Sons, 1967
- /Jel03/ **Mohieddine Jelali and Andreas Kroll**, *Hydraulic Servo-systems: Modeling, Identification and Control*, Springer, 2003
- /Eat99/ **Eaton Corp.** *Proportional Valve Manual*, 1999
- /Eat92/ **Eaton Corp.** Training Center, *Industrial Hydraulics Manual*, 1992
- /Yua05/ **QingHui Yuan and Jae Y Lew**, *Modeling and control of two stage twin spool servo-valve for energy-saving*, American Control Conference, 2005, 8-10 June 2005 Page(s): 4363 - 4368 vol. 6
- /Wu03/ **Duqiang Wu, Richard Burton and Greg Schoenau**, *An empirical discharge coefficient model for orifice flow*, International Journal of Fluid Power, Vol. 4, No. 1, Apr 2003.
- /Lev96/ **William S. Levine**, *The Control Handbook*, CRC press LLC, 1996